Reconciling molecular regulatory mechanisms with noise patterns of bacterial metabolic promoters in induced and repressed states

Matthew L. M. L. Ferguson, Dominique D. Le Coq, Matthieu M. Jules, Stephane S. Aymerich, Ovidiu O. Radulescu, Nathalie N. Declerck, Catherine A. C. A. Royer

▶ **To cite this version:**

Matthew L. M. L. Ferguson, Dominique D. Le Coq, Matthieu M. Jules, Stephane S. Aymerich, Ovidiu O. Radulescu, et al.. Reconciling molecular regulatory mechanisms with noise patterns of bacterial metabolic promoters in induced and repressed states. Proceedings of the National Academy of Sciences of the United States of America, 2012, 109 (1), pp.155 - 160. 10.1073/pnas.1110541108 . hal-01004232

HAL Id: hal-01004232
https://hal.science/hal-01004232

Submitted on 29 May 2020

HAL is a multi-disciplinary open access archive for the deposit and dissemination of scientific research documents, whether they are published or not. The documents may come from teaching and research institutions in France or abroad, or from public or private research centers.

L'archive ouverte pluridisciplinaire **HAL**, est destinée au dépôt et à la diffusion de documents scientifiques de niveau recherche, publiés ou non, émanant des établissements d'enseignement et de recherche français ou étrangers, des laboratoires publics ou privés.

Distributed under a Creative Commons Attribution 4.0 International License

Reconciling molecular regulatory mechanisms with noise patterns of bacterial metabolic promoters in induced and repressed states

Matthew L. Ferguson[a], Dominique Le Coq[b,c,d], Matthieu Jules[b,d], Stéphane Aymerich[b,d], Ovidiu Radulescu[e], Nathalie Declerck[a,f,1], and Catherine A. Royer[a,1]

[a]Centre de Biochimie Structurale, Institut National pour la Santé et la Recherche Médicale U554, Centre National pour la Recherche Scientifique Unité Mixte de Recherche 5048, Université Montpellier 1 and 2, F-34090 Montpellier, France; [b]Institut National pour la Recherche Agronomique, Unité Mixte de Recherche 1319 Micalis, F-78350 Jouy-en-Josas, France; [c]Centre National pour la Recherche Scientifique, F-78350 Jouy-en-Josas, France; [d]AgroParisTech, Unité Mixte de Recherche Micalis, F-78350 Jouy-en-Josas, France ; [e]Dynamique et Interactions des Membranes Normales et Pathologiques-Unité Mixte de Recherche 5235 Centre National pour la Recherche Scientifique, Université Montpellier 1 and 2, F-34095 Montpellier, France; and [f]Institut National pour la Recherche Agronomique Département de Microbiologie, F-75338 Paris, France

Edited by Eric Dean Siggia, The Rockefeller University, New York, NY, and approved October 21, 2011 (received for review July 7, 2011)

Assessing gene expression noise in order to obtain mechanistic insights requires accurate quantification of gene expression on many individual cells over a large dynamic range. We used a unique method based on 2-photon fluorescence fluctuation microscopy to measure directly, at the single cell level and with single-molecule sensitivity, the absolute concentration of fluorescent proteins produced from the two *Bacillus subtilis* promoters that control the switch between glycolysis and gluconeogenesis. We quantified cell-to-cell variations in GFP concentrations in reporter strains grown on glucose or malate, including very weakly transcribed genes under strong catabolite repression. Results revealed strong transcriptional bursting, particularly for the glycolytic promoter. Noise pattern parameters of the two antagonistic promoters controlling the nutrient switch were differentially affected on glycolytic and gluconeogenic carbon sources, discriminating between the different mechanisms that control their activity. Our stochastic model for the transcription events reproduced the observed noise patterns and identified the critical parameters responsible for the differences in expression profiles of the promoters. The model also resolved apparent contradictions between in vitro operator affinity and in vivo repressor activity at these promoters. Finally, our results demonstrate that negative feedback is not noise-reducing in the case of strong transcriptional bursting.

B. subtilis | central carbon metabolism | promoter activity | stochastic gene expression | gene expression control

Gene expression and regulation exhibit a high degree of stochasticity when studied at the level of individual cells. Even in genetically identical cell populations exposed to a uniform environment, gene activity levels and their phenotypic consequences are subject to random fluctuations that generate cell-to-cell variations and eventually lead to alternative cell fates. This stochastic "noise" in gene expression is thought to be a critical, biologically relevant property of genetic circuits in both microbial and eukaryotic cells (1–3). Noise in gene expression primarily originates from bursting of mRNA production and mRNA translation into proteins. Gene promoters stochastically switch between "off" states with no mRNA produced and sharp production during "on" states. The burst size and frequency are thus two key parameters of stochastic protein expression at the single cell level (4–6). At the molecular level, the specific mechanisms of transcription and translation and, if relevant, the associated regulatory mechanisms, generate different patterns and levels of noise. Gene expression noise patterns are thus expected to be under selection by evolution. Several indirect and direct lines of evidence for counterselection of noise in expression of genes important for cell growth have been reported (7, 8), and a quantitative estimation of the general deleterious effect of noise has been recently proposed (9). However, elevated expression noise is advantageous in the context of particular biological processes such as development (10) or for specific classes of genes (11). In the context of environmental changes, expression noise enabling stochastic phenotype switching can be used by cells or cell populations as effective adaptation strategies (12, 13). Expression noise can also provide insights into gene function (14) or critical aspects of the molecular mechanism that control the expression of a particular gene.

In the present work we investigated gene expression noise patterns in a natural coherent genetic system in bacteria and a simple adaptation process—namely, the central carbon metabolism (CCM) in the model Gram positive bacterium *Bacillus subtilis* and a switch in carbon source. At the molecular level, we focused on the transcription initiation step of the genetic expression process. Within the CCM network, we characterized promoter activity at main control points in the physiological switch between glycolysis and its reverse pathway, gluconeogenesis, which allows for growth on noncarbohydrate carbon sources. In *B. subtilis*, this switch involves two glyceraldehyde 3-phosphate dehydrogenases, GapA and GapB, that catalyze opposite reactions, and the phospho*enol*carboxykinase, PckA, that catalyses another irreversible gluconeogenic reaction under physiological conditions (Fig. 1*A*) (15, 16). The auto-repressed *gapA* operon, encoding its repressor CggR, GapA as well as four other central glycolytic enzymes, is induced under glycolytic conditions upon binding of fructose-1,6-bis-phosphate (FBP), a metabolite of glucose, to CggR (17). The operator site for CggR is located downstream of the transcription start site and upstream of the translation initiation region (RBS), and hence CggR is thought to function as a roadblock to the transcribing RNA Polymerase (RNAP) (17, 18). The GapB and PckA enzymes are both required for the utilization of gluconeogenic carbon sources, such as malate, but their expression is deleterious under glycolytic regimes (15, 16, 19). CcpN is the repressor responsible for the very strong catabolite repression of the *gapB* and *pckA* promoters in the presence of glucose or other glycolytic substrates (16). It plays a dominant role in the control of carbon fluxes through central metabolic pathways in *B. subtilis* and is obligate for opti-

Author contributions: S.A., N.D., and C.A.R. designed research; M.L.F., D.L.C., M.J., and N.D. performed research; M.L.F., D.L.C., M.J., O.R., N.D., and C.A.R. analyzed data; S.A., O.R., N.D., and C.A.R. wrote the paper.

The authors declare no conflict of interest.

This article is a PNAS Direct Submission.

[1]To whom correspondence may be addressed. E-mail: catherine.royer@cbs.cnrs.fr or nathalie.declerck@cbs.cnrs.fr.

This article contains supporting information online at www.pnas.org/lookup/suppl/doi:10.1073/pnas.1110541108/-/DCSupplemental.

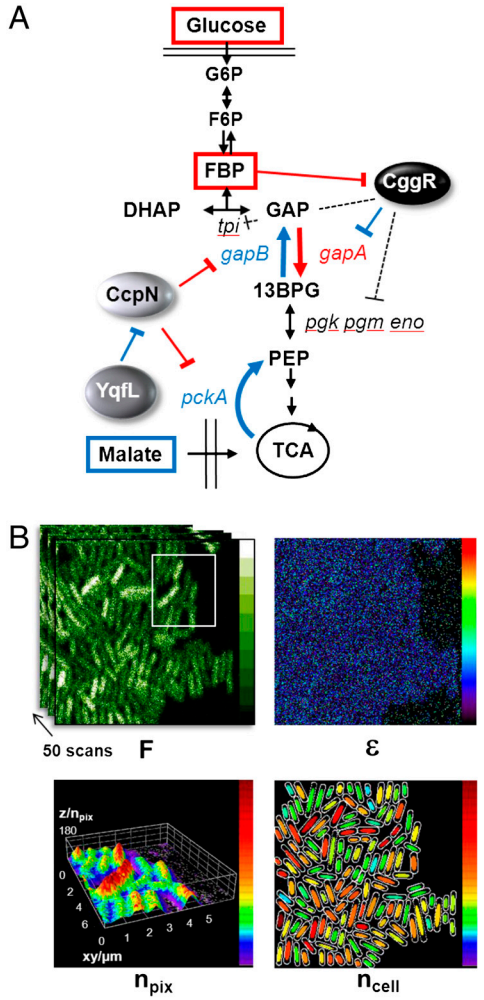

Fig. 1. (*A*) Schematic of the central carbon metabolism showing the switch between glycolysis and gluconeogenesis controlled by the repressors CggR and CcpN. Important metabolites are in squares, regulatory proteins are ellipses, and the genes coding for the enzymes are in small italic letters. When glucose is available for cell growth, fructose-1,6-biphosphate (FBP) accumulates and blocks the repressive action that CggR exerts on the transcription of *gapA* and four other central glycolytic genes (*pgk*, *pgm*, *eno*, and *tpi*). Because CggR is transcribed from the same *gapA* operon that it represses, it is also an autorepressor. Inversely, when cells are grown on malate or other nonglycolytic carbon sources, the CcpN repressor is inhibited by an unknown mechanism involving YqfL, allowing expression of the essential gluconeogenic genes *gapB* and *pckA*. (*B*) Schematic of 2psN&B experiments. A stack of 50 raster scans of agarose immobilized live cells of *B. subtilis* expressing *gfpmut3* are recorded using infrared (930 nm) laser excitation and a dwell time of 50 μs at each pixel (faster than GFP diffusion); full scale of fluorescence intensity (*F*) is 10 photon counts/pixel/50 μs laser dwell time. The fluorescence fluctuations relative to the mean at each pixel are used to calculate the pixel-based maps of the true (shot noise corrected) molecular brightness (ε, full scale 1 photon/molecule/50 μs dwell time) and the number (n_{pix}) of the fluorescent particles detected in the 2-photon excitation volume (vol_{ex} = 0.07 fL inside *B. subtilis*); a 3D surface plot of n_{pix} is shown for the white-delineated area of the above intensity panel. Bottom right: Cartoon representation of the individual cells auto-detected using PaTrack (40) and showing the 50% central pixels used for averaging the particles number in each cell (n_{cell}); the full scale for the n_{pix} and n_{cell} maps is 180 molecules/vol_{ex}.

mal growth under glycolytic conditions (16, 19). CcpN activity is linked to the energy charge of the cell (20) and is also negatively controlled by the coexpressed regulatory protein, YqfL (16). The CcpN operator site overlaps the promoter region of the *gapB* gene, but the bound repressor does not hamper RNAP binding. Rather, CcpN is thought to act on transcription initiation by preventing promoter escape by RNAP (20, 21).

Assessing noise in gene expression in order to obtain molecular mechanistic insights concerning its physical origins requires accurate quantification of expression levels in hundreds of individual cells over a large dynamic range, under repressing as well as inducing conditions, and in particular at very low levels of expression where stochastic effects are expected to be most prominent. The fluorescent protein intensity measurements provided by the standard approaches typically used in such studies yield only fluorescence intensity values which are related to concentration by an unknown scaling factor. Moreover, the sensitivity of such measurements is restricted by the relatively high auto-fluorescence of the bacterial cell cytoplasm. Hence, measuring the activity of weakly transcribed genes using fluorescent protein reporter systems is usually not possible (2). Although recent approaches extend the range of the intensity-based methods to the single-molecule level (22–24), they remain indirect and suffer from uncertainty in molecular brightness and background fluorescence. Here we applied a modified version of two-photon scanning (true) number and brightness (2psN&B) (25, 26), in which the intensity fluctuations at each pixel in a series of rapid raster scanned images of bacteria are used to deconvolve the average intensity (counts/s) into the molecular brightness (counts/s/molecule) and absolute number (molecules) of fluorescent proteins diffusing inside individual bacterial cells (Fig. 1*B*) (27). Thus unlike standard imaging techniques, which yield fluorescence intensity, sN&B provides absolute concentrations and can be carried out using confocal microscopy, although with more autofluorescence and photo-bleaching (Fig. S1) than with the 2-photon excitation used here.

Using this approach, our primary objective was to focus on promoter activity. We sought to directly measure in single cells transcriptional activity of key regulated promoters in their repressed and derepressed states to characterize any heterogeneity among the cell population and to understand how cells are prepared for environmental changes. Moreover we sought to measure transcriptional bursting and to reveal how control mechanisms at these different promoters affect the frequency and the size of the transcriptional bursts during the switch between inactive and active states. Finally, we asked whether, using stochastic models of the molecular control mechanisms of the studied promoters, we could correlate the operative mechanistic physical features with specific characteristics of the noise patterns.

Results

Absolute Quantification of Expression Levels Under Permissive and Repressing Conditions. Using N&B analysis we measured the absolute concentration of green fluorescent protein (GFP) in individual cells expressing *gfpmut3* (encoding a very bright, fast-maturing and stable GFP variant) (28) from four promoters of interest, P_{cggR} (*gapA* operon), P_{gapB}, P_{pckA}, and P_{ccpN}, (Fig. S2) grown at steady state under glycolytic (glucose) or gluconeogenic (malate) conditions. Fluorescent particles number maps and histograms of the distributions in the bacterial populations (Fig. 2 *A* and *B*) were calculated as described in detail elsewhere (27) (*SI Text*). Large differences in the expression levels and cell-to-cell variations were observed for the different strains depending on the carbon source used for growth. The P_{cggR}*gfp* fusion was strongly expressed on glucose but poorly repressed on malate, exhibiting an induction level of only sevenfold, in good agreement with bulk population measurements using *gfpmut3* (Fig. S3) or other reporter systems (17). Expression from the P_{cggR} promoter was visibly heterogeneous for the cell population grown on malate (Fig. 2*A*). The number of fluorescent particles detected in our 2p excitation volume inside the bacterial cell, vol_{ex} (approximately 0.07 fL) ranged from 30 to over 250 (Fig. 2*B*). In contrast, transcription from both P_{gapB} and P_{pckA} was very strongly re-

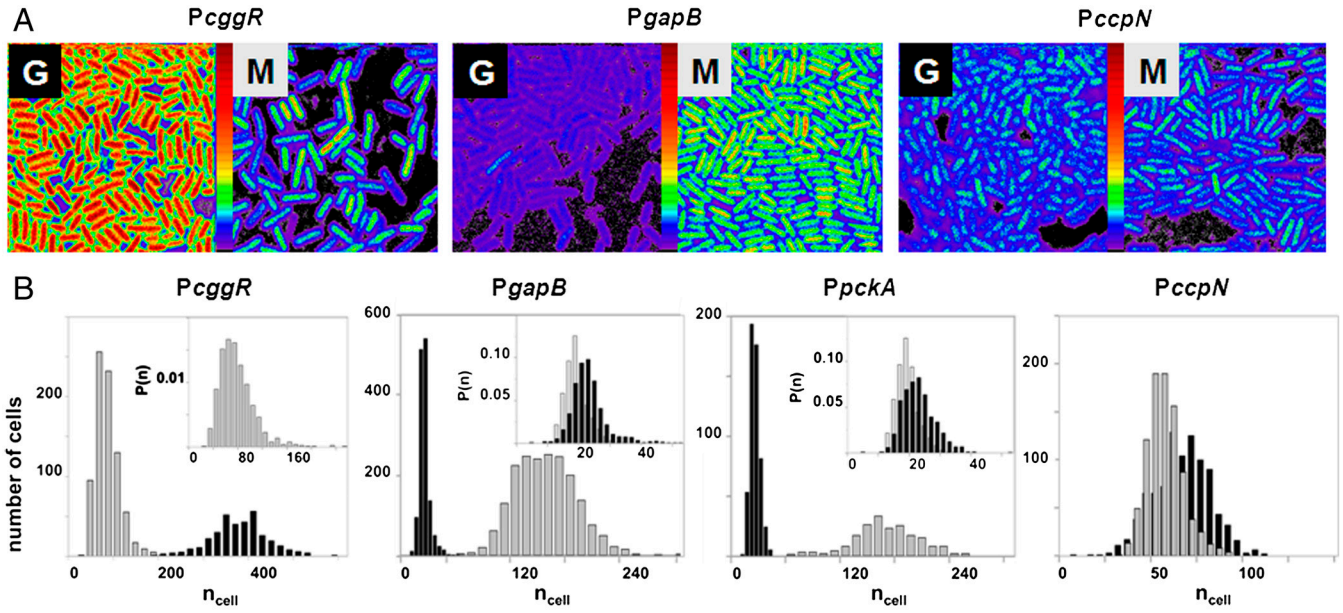

Fig. 2. Cell-by-cell quantification of catabolite regulation in *B. subtilis* by 2psN&B. (*A*) Pixel-based fluorescent particles number maps of *B. subtilis* cells expressing *gfpmut3* transcriptional fusion from P_{ccgR}, P_{gapB} (results are similar for P_{pckA}; not shown), and P_{ccpN}. Cells harvested from liquid cultures containing 0.5% glucose (G) or 0.5% malate (M) as the sole carbon source were immobilized on agarose pads for 2psN&B analysis as described in Fig. 1*B*. The full scale is 360 molecules/vol_{ex}. (*B*) Cell-based particles number (n_{cell}) distributions for the indicated promoter-*gfpmut3* fusion strains grown on glucose (black) or malate (gray). Inset in the first panel shows the expanded histogram of the probability density function $P(n_{cell})$ measured in malate for P_{cggR}. Insets in panel 2 and 3 show the expanded histogram of the probability density function $P(n_{cell})$ observed in glucose for the P_{gapB} and P_{pckA} promoters in black, and that observed for the background BSB168 strain in gray.

pressed on glucose and induced over 40-fold on malate (Fig. 2 *A* and *B*, middle panels). For these promoters under repressing condition, we were able to determine a population average of approximately 3.5 GFP molecules (per vol_{ex}) above the background of dim fluorescent particles observed in the reference BSB168 receiver strain (Fig. 2*B*, insets of panel 2 and 3). This corresponds to a population average concentration of approximately 80 nM or around 30–50 total GFP molecules in the bacterial cells, depending upon their size. For the strain carrying the *gfpmut3* fusion with the weak and constitutive P_{ccpN} promoter we measured rather low GFP concentrations, averaging approximately 1 μM on both carbon sources.

Changes in Noise Pattern Parameters During Nutrient Shifts. The coefficient of variation (COV), one of the metrics used for quantifying noise in gene expression, is the ratio of the standard deviation in the number of proteins (/vol_{ex}) over the mean, $\sigma_n/\langle n\rangle$, for distributions in a population of bacteria (i.e., Fig. 2*B*). For all three regulated promoters (P_{cggR}, P_{gapB}, and P_{pckA}), the COV is very large (approximately 60–100%) for the repressed promoters. The increase in the average number of GFP molecules under permissive conditions is accompanied by a drastic decrease in $\sigma_n/\langle n\rangle$ (Fig. 3*A*) but remains above the experimental uncertainty inherent to our method (approximately 0.05) (27). For the unregulated P_{ccpN} promoter, we observed no significant change in the $\sigma_n/\langle n\rangle$ value upon the shift of carbon source. We note that a small coefficient of variation does not necessarily mean that the noise is small; this is particularly true for skewed and leptokurtic histograms, such as that observed for P_{cggR}, and which are usually associated with bursting (2, 5, 29).

Two other key parameters of stochastic gene expression can be extracted from the average and variance of GFP molecules in the cell population histograms: the apparent frequency of protein production burst per cell cycle ($a = \langle n\rangle^2/{\sigma_n}^2$) and the average number of protein molecules produced per burst, related to the Fano factor ($b = {\sigma_n}^2/\langle n\rangle$) (5). Thus, for a repressible promoter, the mean expression level, $\langle n\rangle = ab$, can be decreased by reducing a or b or both. We note that in our system, differences in bursting characteristics from one promoter fusion to another and from one condition to another only emanate from transcriptional bursting. Indeed, in all our constructions, the *gfpmut3* gene is under identical translational signal, insensitive to the different physiological conditions examined here. As expected for the constitutive promoter, P_{ccpN}, little variation is observed in either the values of a or b upon a switch in carbon source. In contrast, examination of the variations in these parameters for the glycolytic and gluconeogenic promoters on different carbon sources (Fig. 3*B*) reveals dramatic differences between their noise patterns. Indeed the parameters, a and b, are very dynamic and discriminative of the behavior of the two types of promoters, providing strong evidence that the major contribution to the observed cell-to-cell fluctuations is intrinsic to the regulatory circuitry. The gluconeogenic promoters (P_{gapB} and P_{pckA}) show a strong relative decrease of both burst size and frequency upon repression under glucose, whereas upon repression of P_{cggR} under malate, a decreases significantly while b actually increases slightly. Large bursts under repression by CggR are thus responsible for the heterogeneity observed in this population (Fig. 2*A*). Our findings reveal two distinct noise signatures associated with the glycolytic as opposed to gluconeogenic promoters.

Modeling the Expression Patterns of P_{cggR} and P_{gapB} During the Nutrient Shift. We modeled the kinetics of the transcription events from the P_{cggR} and P_{gapB} promoters with a unique realistic scheme inspired from a generic model for prokaryotic gene expression (30) (Fig. 4 *A*–*B* and Table S1). An in-depth justification for fixed parameter values and fitting procedure is given in *SI Methods*. Our model included repressor binding and dissociation from the operator DNA, ${k_1}^{on}$ and ${k_1}^{off}$, respectively. The main contribution to the fluctuations of mRNA production and of the other downstream variables arose from dissociation of the repressor, which justifies a two-state operator model. Transcription initia-

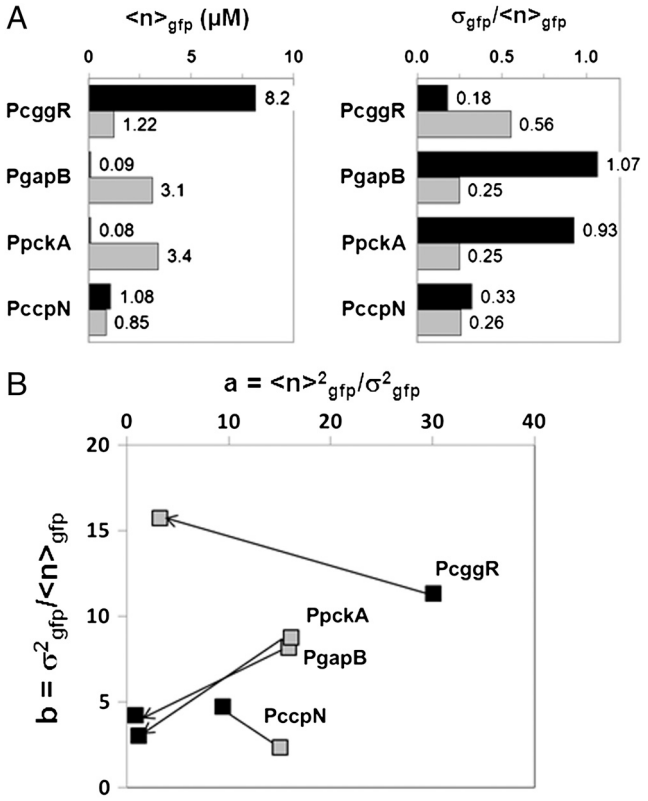

Fig. 3. Changes in promoter activity levels and noise patterns upon a switch of carbon source. (*A*) The average number of GFPmut3 molecules per vol_{ex} ($\langle n\rangle_{gfp}$ expressed in micromolar concentration) and its coefficient of variation (the standard deviation over the mean, $\sigma_{gfp}/\langle n\rangle_{gfp}$) in the cell populations grown on glucose (black bars) or malate (gray bars), estimated from the cell-based particles number distributions shown in Fig. 2*B* and considering a fixed auto-fluorescence background contribution as determined in the BSB168 receiver strain under identical experimental conditions. (*B*) Effect of nutrient switch on promoter activity noise patterns. The parameter of stochastic gene expression, the Fano factor b ($\sigma^2_{gfp}/\langle n\rangle_{gfp}$), related to GFP production burst size is plotted against a ($\langle n\rangle^2_{gfp}/\sigma^2_{gfp}$) related to the GFP production burst frequency for the activity of the indicated promoters on glucose (black square) or malate (gray diamonds). The single arrows indicate the sense of repression for the regulated promoters.

tion was assigned rate constants k_2 or k'_2, and the transcribing polymerase (tRNAP) was considered to synthesize the mRNA leader region containing the RBS with rate constants k_3 (30, 31) or k'_3, depending on whether the operator DNA is free or bound by repressor. A switched, first order reaction of rate constant k_4 was used to model dissociation of the elongation complex, thus reducing jamming of stalled polymerase molecules in the repressor-bound operator state for P_{cggR}. We pooled several states (29, 31, 32) related by rapid transitions and consider that RBS gives rise directly to the ribosome elongating the protein chain (ElRib) then to the matured GFP (MdGFP). All reactions past RBS synthesis are considered to be identical for the promoters under study. We adjusted the parameters of the model to fit the experimental expression histograms.

The model reproduces well the observed behavior of P_{gapB} and P_{cggR} (Fig. 4*C* and Table S1). Testing key parameters for their uniqueness revealed significant constraints on their values (*SI Methods* and Fig. S4). The promoters function in a regime where $k_1^{off}/k_1^{on[R]}$ is small for all conditions and promoters; the probability, $1-p$, that the repressor, R, is bound to the DNA remains large, and repression does not vanish even under permissive conditions, in good agreement with genetic data showing constitutive overexpression of these promoters in repressor knockout strains (15, 16). The nutrient switch affects repression mainly at two levels: affinity of the repressor for the DNA (k_1^{off}) in the case of P_{cggR} and concentration of active repressor and hence the burst duration and size ($1/k_1^{on}[R]$) in the case of P_{gapB}. Good fits for these two promoters were constrained by the modification of these two parameters, respectively. At P_{gapB}, a decrease in the concentration of active repressor is consistent with the proposed sequestration of CcpN by YqfL under malate, although the total CcpN concentration is not thought to change (16). The change of k_1^{off} is minimal upon induction, and hence K_D values are constant and in the range of 0.8 nM, in reasonable agreement with the 8 nM affinity measured in vitro (33, 34). For CggR, operator affinity is high under repression, $K_D = 0.1$ nM, and decreases about 10-fold upon induction (k_1^{off} increases), in reasonable agreement with the in vitro operator affinity (<0.5 and 10 nM) of CggR in absence and presence of inducer (35, 36). The model reconciles as well this high in vitro affinity with moderate repression by CggR in vivo (15). The position of the CggR operator site between the promoter and the RBS allows unhindered RNAP binding and initiation and hence passage of multiple polymerase molecules while the repressor is dissociated, leading to large amplitude bursts. Indeed, the large bursts for P_{cggR} under repression cannot be modeled otherwise. Moreover, the enzymes of the CCM must be produced in large quantities when needed, and hence we must assume strong promoters in order to insure this strong production in the derepressed state. The price to pay is that strong promoters favor transcriptional bursting. In addition, strong bursting under repression for P_{cggR} is favored by the fact that CggR is a self-repressed promoter, and hence the concentration of repressor is lower under repressive, relative to permissive, conditions.

Discussion

Our N&B data provide reliable measurements of absolute gene expression levels and fluctuations from metabolic promoters implicated in catabolite repression under both permissive and repressive conditions. The activity of the strongly repressed gluconeogenic promoters has been undetectable at the single cell level by other methods. Indeed, combined two-photon excitation and raster scanning considerably reduce both the auto-fluorescence from the bacterial cytoplasm and photo-bleaching of the GFP molecules, thereby achieving the single-molecule detection limits required for single cell quantification of gene expression levels from these strongly repressed promoters. Moreover, fluorescence fluctuation-based methods such as N&B analysis do not require calibration of the light intensity signal and therefore allow for the direct counting of fluorescent reporter proteins diffusing in the excitation volume.

Our measurements, due to their absolute nature, reveal distinct noise patterns for the glycolytic and gluconeogenic promoters, which inform on the adaptive strategy selected by evolution. For P_{cggR}, 2psN&B allowed us to demonstrate significant cell-to-cell heterogeneity, in particular the existence of a subpopulation of cells expressing GFP under the repressed state at levels as high as half the average level of induced cells. This heterogeneity does not correspond to bistability that would provoke a bimodal distribution of the expression levels as reported for other bacterial regulation systems (37), instead of the skewed unimodal distribution observed here. Rather it arises from strong transcriptional bursting from this promoter under repression, which itself has two origins. First, P_{cggR} is intrinsically a strong promoter, a required feature for the enzymes of the central carbon metabolism which must be produced in large quantity in the induced state. Secondly, the repressive mechanism of CggR, rather than competing with RNA polymerase for promoter binding, as in the case of the lactose repressor for example, acts as a roadblock to elongation. Hence multiple RNAP molecules can accomplish transcription during repressor dissociation episodes. While the affinity of CggR for its operator is quite high in vitro (35, 36), it

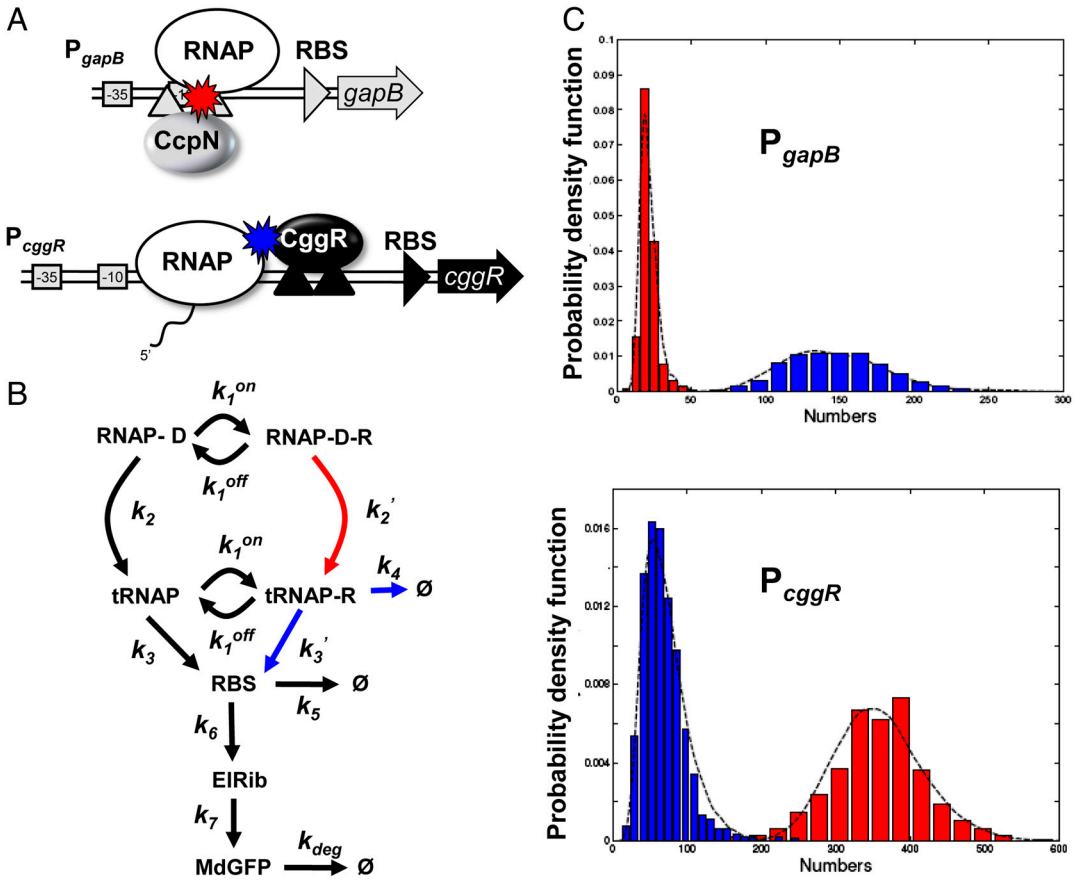

Fig. 4. Model of gene regulation by CggR and CcpN. (*A*) Scheme describing the architecture of the *B. subtilis* P_{ccgR} and P_{gapB} promoter region (boxed −10 and −35 RNAP recognition sequences) and tandem operator sites (black or gray upward triangles) for the CggR or CcpN repressors. Under glycolytic conditions, CcpN is thought to prevent promoter clearance by the RNA polymerase whereas under gluconeogenic conditions CggR acts as a roadblock to the transcribing polymerase when bound as a compact tetramer. (*B*) General model of prokaryotic gene expression and regulation applied to both repressors. RNAP-D is the RNAP-bound DNA, R the active repressor, tRNAP the elongating transcription complex, RBS the ribosome binding site on the transcribed mRNA, ElRib the elongating translation complex, and MdGFP the folded and matured green fluorescent protein. According to the above mechanistic models of regulation, besides changes in DNA affinity constants ($Kd_1 = k_1^{off}/k_1^{on}$), CcpN repression affects primarily k_2, the rate at which the elongation complex is formed, whereas CggR would affect the transcription rate in the mRNA leader region (k_3), thereby increasing the dissociation rate of the (paused) polymerase (k_4). In the *gfpmut3* reporter system used in this study, all steps past RBS production are identical for all promoter constructs and all conditions. The GFPmut3 variant has been shown to be fast-maturing (within a few minutes) and slow degrading (stable for several hours) in *B. subtilis* (3), therefore the degradation rate k_{deg} corresponds to slow dilution whereas the lifetime of the mRNA is much shorter (i.e., $k_5 \gg k_{deg}$). (*C*) Results of the model compared to the experimental data for the stochastic expression of $P_{gapB}gfp$ and $P_{cggR}gfp$ transcriptional fusions under glucose (red) or malate (blue). Lines correspond to the continuous distributions obtained from the model parameters reported in Table S1. The histogram from the $P_{gapB}gfp$ promoter fusion data was not corrected for the BSB168 background contribution, as the deconvolution cannot be done reliably for experimentally reasonable dataset sizes; instead, a Gamma random variable having the same first two moments as the background contribution has been added to the model predictions.

exhibits moderate repressor activity in vivo (17), as it is subject to strong transcriptional bursting. Although transcriptional bursting has been observed, albeit rarely, in prokaryotes (2, 38), quantitative and mechanistic insights into the process, such as those presented here, have been lacking. Significant activity for the P_{cggR} promoter in a subpopulation of cells grown on malate enables them to respond more rapidly when glucose becomes available, thereby conferring a competitive advantage to the clonal population. The high level of noise for this promoter may have been selected for implementing such a bet-hedging adaptation strategy.

As often invoked (39) one is inclined to expect that negative feedback reduces noise. Our results provide the experimental demonstration that this property is not valid in the strong bursting regime of the self-repressed P_{cggR} promoter. Indeed, the burst size scales with the lifetime of the active state of the operator, which for a self-repressed promoter, scales inversely with the concentration of repressor and is smaller under permissive conditions when the feedback is weak. In contrast to the strong transcriptional bursting observed for the glycolytic promoter, in the case of the gluconeogenic promoters, because derepression under glycolytic conditions greatly impairs growth (16, 19), strict control by CcpN and limited noise are essential. Hence, the repressive mechanism of CcpN has evolved to limit bursting in the repressed state by impairing promoter escape by the RNAP, leading to very strong catabolite repression.

In conclusion, our study demonstrates that N&B analysis can be applied for direct and absolute quantification of promoter activity and noise in bacterial populations upon changes in conditions. The highly quantitative nature of our approach, coupled with its sensitivity and broad dynamic range render 2psN&B particularly well suited to the study of promoter activity. Here it allowed us, in a natural bacterial system, to associate expression noise patterns with specific features of molecular mechanisms of transcriptional repression, to demonstrate transcriptional bursting and to show that negative feedback control does not necessarily reduce noise. Hence, 2psN&B offers broad perspectives for the quantitative characterization of a wide range of gene regulatory networks in both prokaryotes and eukaryotes.

Materials and Methods

Bacterial Strains, Cultures, and Sample Preparation. Strains of *Bacillus subtilis* carrying transcriptional fusions with the *gfpmut3* reporter gene were constructed using the pBaSysBioII plasmid designed for high throughput analysis of promoter activities by Live Cell Arrays (3) (http://www.basysbio.eu). (See Fig. S2 and *SI Text* for more details.) Microscopy samples were prepared with cells from exponentially growing cultures and immobilized on 1.5% agarose pads as described in *SI Text* and in ref. 27.

Two-Photon Scanning Microscopy. In scanning N&B analysis the number and molecular brightness of the diffusing fluorescent molecules are calculated from the fluctuations in fluorescence intensity at each pixel in a series of raster scanned images, in which the laser dwell time is small with respect to the diffusion time of the molecule. Fluorescence fluctuations from the average intensity arise from Brownian diffusion into and out of the very small two-photon excitation volume ($vol_{ex} = 0.07$ fL) focused inside the bacterial cells. The pixel-based temporal average and variance images were calculated from 50 raster scans, then the true (shot noise corrected) molecular brightness, ε, was determined at each pixel. The average true molecular brightness $\langle\varepsilon\rangle$ was determined for all of the cells in the field of view using only those central pixels for which the vol_{ex} is encompassed within the cells. This spatially averaged true molecular brightness for each field of view allowed for the calculation of the number of molecules, $n_{pix}\langle/vol_{ex}\rangle$, at each pixel. Then for each cell in the field of view, n_{pix} was averaged over the pixels situated in an ellipse representing the central 50% of the cell area, yielding n_{cell}. The averaged intracellular concentration of GFPmut3 molecules ($\langle n\rangle_{gfp}$) and their intrinsic brightness ($\langle\varepsilon\rangle_{gfp}$) for a population of cells under a particular set of conditions were obtained by correcting the average values obtained from the distribution for background fluorescence from the BSB168 receiver strain bearing no *gfp*. More details on our 2psN&B method are given in *SI Text* and ref. 27.

Modeling. The model of stochastic gene expression is described by the set of biochemical reactions given in Fig. 4*B* and Table S1. We used Gillespie direct simulation accelerated by cycle averaging (29) to compute the stationary solutions of the chemical master equation. The model predictions were compared to the experimental histograms for the *cggR* and *gapB* promoters, under two nutritional conditions, glycolytic (glucose) and gluconeogenic (malate). Parameter values were approximated using analytical approximations for the first two moments of the predicted expression distribution and then refined by minimizing the distance between predicted and observed histograms. Further description of the genetic switch modelling is available in *SI Text*.

ACKNOWLEDGMENTS. The authors would like to thank Caroline Clerté for her assistance in student training on the microscope and Nicole Lautredou and Julien Cau of Montpellier Rio Imaging for their assistance with the confocal microscope. The work was supported by a grant from the Agence Nationale pour la Recherche (ANR-09-BLAN-0285) and by European Union BaSysBio Grant LSHG-CT-2006-037469. M.L.F was supported by postdoctoral fellowships from the National Science Foundation (OISE:IRFP #0710816), European Molecular Biology Organization (ALTF 660-2008), and the European Commission (Marie Curie IIF#237835-InVivoTrnsReg).

1. Eldar A, Elowitz MB (2010) Functional roles for noise in genetic circuits. *Nature* 467:167 173.
2. Kaufmann BB, Van Oudenaarden A (2007) Stochastic gene expression: from single molecules to the proteome. *Curr Opin Genet Dev* 17:107–112.
3. Botella E, et al. (2010) pBaSysBioII: An integrative plasmid generating *gfp* transcriptional fusions for high-throughput analysis of gene expression in *Bacillus subtilis*. *Microbiology* 156:1600–1608.
4. Cai L, Friedman N, Xie XS (2006) Stochastic protein expression in individual cells at the single molecule level. *Nature* 440:358–362.
5. Friedman N, Cai L, Xie XS (2006) Linking stochastic dynamics to population distribution: an analytical framework of gene expression. *Phys Rev Lett* 97:168302.
6. Raj A, et al. (2006) Stochastic mRNA synthesis in mammalian cells. *PLoS Biol* 4:e309.
7. Lehner B (2008) Selection to minimise noise in living systems and its implications for the evolution of gene expression. *Mol Syst Biol* 4:1–5.
8. Newman JR, et al. (2006) Single-cell proteomic analysis of *S. cerevisiae* reveals the architecture of biological noise. *Nature* 441:840–846.
9. Wang Z, Zhang J (2011) Impact of gene expression noise on organismal fitness and the efficacy of natural selection. *Proc Natl Acad Sci USA* 108:E67–E76.
10. Losick R, Desplan C (2008) Stochasticity and cell fate. *Science* 320:65–68.
11. Zhang Z, Qian W, Zhang J (2009) Positive selection for elevated gene expression noise in yeast. *Mol Syst Biol* 5:299.
12. Kussell E, Leibler S (2005) Phenotypic diversity, population growth, and information in fluctuating environments. *Science* 309:2075–2078.
13. Schultz D, et al. (2009) Deciding fate in adverse times: sporulation and competence in *Bacillus subtilis*. *Proc Natl Acad Sci USA* 106:21027–21034.
14. Rinott R, Jaimovich A, Friedman N (2011) Exploring transcription regulation through cell-to-cell variability. *Proc Natl Acad Sci USA* 108:6329–6334.
15. Fillinger S, et al. (2000) Two glyceraldehyde-3-phosphate dehydrogenases with opposite physiological roles in a nonphotosynthetic bacterium. *J Biol Chem* 275: 14031–14073.
16. Servant P, Le Coq D, Aymerich S (2005) CcpN (YqzB), a novel regulator for CcpA-independent catabolite repression of *Bacillus subtilis* gluconeogenic genes. *Mol Microbiol* 55:1435–1451.
17. Doan T, Aymerich S (2003) Regulation of the central glycolytic genes in *Bacillus subtilis*: Binding of the repressor CggR to its single DNA target sequence is modulated by fructose-1,6-bisphosphate. *Mol Microbiol* 47:1709–1721.
18. Chaix D, et al. (2010) Physical basis of the inducer-dependent cooperativity of the Central glycolytic genes Repressor/DNA complex. *Nucleic Acids Res* 38:5944–5957.
19. Tännler S, et al. (2008) CcpN controls central carbon fluxes in *Bacillus subtilis*. *J Bacteriol* 190:6178–6187.
20. Licht A, Golbik R, Brantl S (2008) Identification of ligands affecting the activity of the transcriptional repressor CcpN from *Bacillus subtilis*. *J Mol Biol* 380:17–30.
21. Licht A, Brantl S (2009) The transcriptional repressor CcpN from *Bacillus subtilis* uses different repression mechanisms at different promoters. *J Biol Chem* 284: 30032–30038.
22. Choi PJ, et al. (2008) A stochastic single-molecule event triggers phenotype switching of a bacterial cell. *Science* 322:442–446.
23. Elf J, Li GW, Xie XS (2007) Probing transcription factor dynamics at the single-molecule level in a living cell. *Science* 316:1191–1194.
24. Taniguchi Y, et al. (2010) Quantifying E. coli proteome and transcriptome with single-molecule sensitivity in single cells. *Science* 329:533–538.
25. Digman MA, et al. (2008) Mapping the number of molecules and brightness in the laser scanning microscope. *Biophys J* 94:2320–2332.
26. Digman MA, et al. (2009) Stoichiometry of molecular complexes at adhesions in living cells. *Proc Natl Acad Sci USA* 106:2170–2175.
27. Ferguson ML, et al. (2011) Absolute quantification of gene expression in individual bacterial cells using two-photon fluctuation microscopy. *Anal Biochem* 419:250–259.
28. Cormack BP, Valdivia RH, Falkow S (1996) FACS-optimized mutants of the green fluorescent protein (GFP). *Gene* 173:33–38.
29. Crudu A, Debussche A, Radulescu O (2009) Hybrid stochastic simplifications for multiscale gene networks. *BMC Syst Biol* 3:1–25.
30. Bar-Nahum G, et al. (2005) A ratchet mechanism of transcription elongation and its control. *Cell* 120:183–193.
31. Kierzek AM, Zaim J, Zielenkiewicz P (2001) The effect of transcription and translation initiation frequencies on the stochastic fluctuations in prokaryotic gene expression. *J Biol Chem* 276:8165–8172.
32. Radulescu O, et al. (2008) Robust simplifications of multiscale biochemical networks. *BMC Syst Biol* 2:1–25.
33. Zorrilla S, et al. (2008) Characterization of the control catabolite protein of gluconeogenic genes repressor by fluorescence cross-correlation spectroscopy and other biophysical approaches. *Biophys J* 95:4403–4415.
34. Licht A, Brantl S (2006) Transcriptional repressor CcpN from *Bacillus subtilis* compensates asymmetric contact distribution by cooperative binding. *J Mol Biol* 364:434–448.
35. Zorrilla S, et al. (2007) Fructose-1,6-bisphosphate acts both as an inducer and as a structural cofactor of the central glycolytic genes repressor (CggR). *Biochemistry* 46:14996–15008.
36. Zorrilla S, et al. (2007) Inducer-modulated cooperative binding of the tetrameric CggR repressor to operator DNA. *Biophys J* 92:3215–3227.
37. Dubnau D, Losick R (2006) Bistability in bacteria. *Mol Microbiol* 61:564–572.
38. Golding I, et al. (2005) Real-time kinetics of gene activity in individual bacteria. *Cell* 123:1025–1036.
39. Becskei A, Serrano L (2000) Engineering stability in gene networks by autoregulation. *Nature* 405:590–593.
40. Espenel C, et al. (2008) Single-molecule analysis of CD9 dynamics and partitioning reveals multiple modes of interaction in the tetraspanin web. *J Cell Biol* 182:765–776.